Mossbauer and magnetic susceptibility studies of the alloy series $FeAl_{1-x}Cu_x$

1990 J. Phys.: Condens. Matter 2 4895

(http://iopscience.iop.org/0953-8984/2/22/010)

J. Phys.: Condens. Matter **2** (1990) 4895–4906. Printed in the UK

Mössbauer and magnetic susceptibility studies of the alloy series $FeAl_{1-x}Cu_x$

M A Kobeissi†, Q A Pankhurst, S Suharan and M F Thomas
Department of Physics, University of Liverpool, Liverpool L69 3BX, UK

Received 29 March 1989, in final form 7 March 1990

Abstract. Magnetic susceptibility and Mössbauer spectroscopy studies were carried out on the alloy series $FeAl_{1-x}Cu_x$ ($0 < x \leqslant 0.4$). The variation of susceptibility with temperature showed transitions from a paramagnetic to a spin glass phase for copper contents $0.15 \leqslant x \leqslant 0.25$. For $x = 0.325$ transitions from a paramagnetic to a ferromagnetic and from a ferromagnetic to a magnetic glass phase were observed as the temperature was decreased. Mössbauer spectra gave information on the microscopic conditions at the iron sites. The electron density at the iron nuclei increased linearly with copper concentration x. Distributions of hyperfine fields were observed for all alloys at 4.2 K and related to iron cluster structure. Comparison between phase transition temperatures obtained by susceptibility and Mössbauer observations gave information on the relaxation of clusters. The size of these clusters as a function of x was studied via a simulation calculation and used to account for the occurrence of a ferromagnetic phase at a critical value of x.

1. Introduction

The magnetic properties of dilute and concentrated transition metal alloys, especially those exhibiting spin glass behaviour, have been the subject of many recent studies [1–20]. Experimental and theoretical results on phase transitions, magnetic or otherwise, at well defined temperatures in these alloys are still subject to different interpretations [17, 21, 22]. The mechanism and nature of the magnetic interactions within the alloys is not yet completely understood [22]. A number of theories based on particular models have been presented but a general description of the magnetic nature and behaviour of such alloys is some way off [7–10, 13, 14]. More experimental work to establish detailed magnetic behaviour shown by these systems is required to provide comprehensive tests of the theoretical models.

One set of alloys of interest in this field is the iron rich Fe/Al series which was among the first to exhibit anomalous magnetic and spin glass behaviour [4, 6]. A number of structural, magnetic and Mössbauer studies have been made on the alloy series $Fe_{2-y}Al_y$ ($0 < y \leqslant 1$) with the aim of accounting for its magnetic structure and its temperature dependence [1–4]. The alloy with $y = 1$, which may be regarded as the parent material of the ternary alloys of this study, crystallises on slow cooling in the ordered B2(CsCl) structure of interpenetrating cubic Fe and Al lattices. The site ordering of this alloy is complete while for $y < 1$ the Fe lattice is complete with excess Fe atoms substituting randomly on the Al lattice [3]. This structurally ordered FeAl does not show a transition

† Present address: Department of Physics, UAE University, Al-Ain, PO Box 15551, United Arab Emirates.

0953-8984/90/224895 + 12 $03.50

to a magnetically ordered state [23] but evidence for such a transition is observed [3] in the alloy with $y = 0.9$. Magnetic studies [4] on the iron rich alloys with $y \sim 0.3$ have demonstrated the occurrence of mictomagnetism (spin glass clusters) and observed a re-entrant ferromagnetic phase for $0.27 \leqslant y \leqslant 0.31$. Several theoretical studies [7–10, 14] have been made to account for the phase diagrams and other magnetic properties of such alloy systems.

The related ternary alloy series $FeAl_{1-x}T_x$, where T is a transition metal atom, widen the variety of systems likely to show related magnetic behaviour. In the series $FeAl_{1-x}Cu_x$, the subject of this study, neutron diffraction studies [12] indicate that the Cu atoms substitute randomly on Fe and Al sublattices causing some transfer of Fe atoms to the Al sublattice. High field magnetisation [16] studies indicate the presence of a ferromagnetic phase when $x \geqslant 0.27$ and cluster formation for $x \geqslant 0.20$. This present study aims to establish a magnetic phase diagram and to complement the macroscopic magnetic results with an investigation of the microscopic environment of the different phases via Mössbauer spectroscopy.

2. Experimental techniques

The alloys used in this investigation were those used in the x-ray and neutron diffraction measurements of Saleh *et al* [12]. Details of the fabrication of these materials and their heat treatment are reported by Okpalugo *et al* [11].

2.1. AC susceptibility measurements

In the measurements of AC susceptibility χ_{AC} the samples were formed by compressing the alloy powder into nylon capillary tubes to form solid compact cylinders of 1.5 mm diameter and 30 mm length. Each sample was held at the centre of the pick-up coil of a previously balanced mutual inductance bridge. AC frequencies of 15 Hz and 30 Hz were used with an RMS AC field of 8 μT. Static fields of up to 12 mT were applied in a geometry where AC and DC fields were parallel to the long axis of the sample. Temperature variation was achieved using a flow cryostat equipped with a temperature control system, incorporating a resistance temperature sensor which stabilised the temperature with an accuracy of better than 0.5 K. In the determination of the freezing and ordering phase transition temperatures T_f and T_c the values of χ_{AC} were recorded over a complete up and down temperature cycle starting with the lowest temperature.

2.2. Mössbauer measurements

Mössbauer absorbers were made by spreading finely powdered alloys on masking tape and enclosing them in nylon sample holders. The spectrometers incorporated sources of ^{57}Co in a rhodium matrix of strengths up to 50 mCi driven in double ramp mode. The folded spectra showed a flat background. The spectrometers were calibrated with thin metallic iron foils at room temperature and isomer shift values are quoted relative to these calibrations.

Mössbauer transition temperatures T_{HF}, indicated by the detection of a magnetic hyperfine field, were determined using the thermal scanning method described by Kobeissi [24]. For alloys in the range $0.05 \leqslant x \leqslant 0.25$ the sample results were obtained in a helium flow cryostat while those for the $x = 0.325$ sample were obtained in a heated

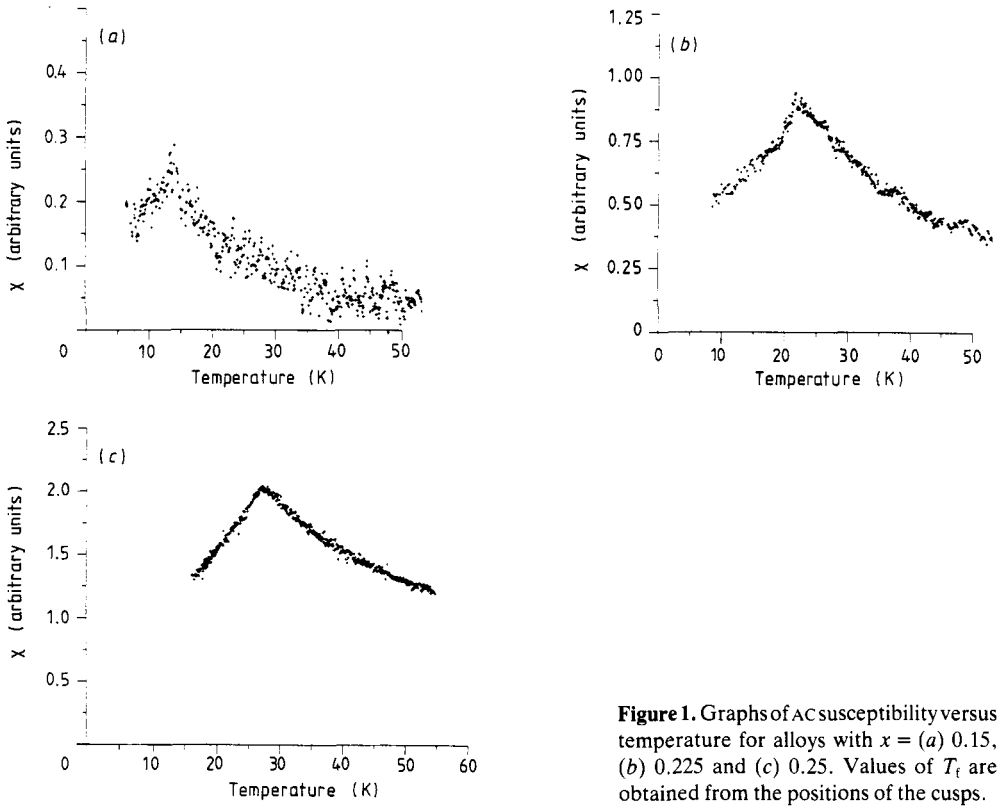

Figure 1. Graphs of AC susceptibility versus temperature for alloys with x = (*a*) 0.15, (*b*) 0.225 and (*c*) 0.25. Values of T_f are obtained from the positions of the cusps.

insert within a liquid nitrogen bath. The magnetic spectra investigating the variation in hyperfine field B_{HF} with composition x, were obtained at 4.2 K in a helium cryostat. These spectra were analysed in terms of a probability distribution of the hyperfine field, $P(B_{HF})$, represented by an unconstrained histogram. An 'integrated' lineshape was used corresponding to the integration of a Lorentzian line over the range of hyperfine fields (and therefore the range of velocities) within each histogram box. Quadrupole splitting was taken to be zero and a linear correlation between increasing isomer shift and decreasing hyperfine field was assumed. This correlation was in line with the picture of electron occupation of the 3d shell in the iron atoms discussed in sections 4.3 and 4.4.

3. Results

3.1. Variation of magnetic susceptibility χ_{AC} with temperature T and copper concentration x

The AC susceptibility measurements were recorded for the alloys having $0.05 \leqslant x \leqslant 0.325$. For $x < 0.15$ the susceptibilities were too small for reliable measurement. Figure 1 shows the variation of χ_{AC} for the alloys with $0.15 \leqslant x \leqslant 0.25$ as a function of temperature and x. The shapes of the χ_{AC} versus T graphs show a distinct cusp, characteristic of spin glass magnets [20]. The peak of the cusp determines the transition temperature T_f from the paramagnetic to spin glass state. It is seen that T_f increases with x. Values of all the transition temperatures are collected in table 1. In other spin

Table 1. Phase transition temperatures. Values of T_f are obtained for $0.15 \leqslant x \leqslant 0.25$ from the sharp cusps observed in the zero field susceptibility measurements. For $x = 0.325$ the values of T_f and T_c are taken from the zero field susceptibility graph at points of maximum modulus of slope. The temperatures T_{HF} corresponding to the appearance of a hyperfine field are obtained from the Mössbauer scanning technique.

Sample x	T_{HF} (K)	T_c (K)	T_f (K)
0.10	13 ± 1	—	—
0.15	17 ± 1	—	13 ± 1
0.225	29 ± 1	—	22 ± 1
0.25	33 ± 1	—	27 ± 1
0.325	273 ± 1	217 ± 5	45 ± 5

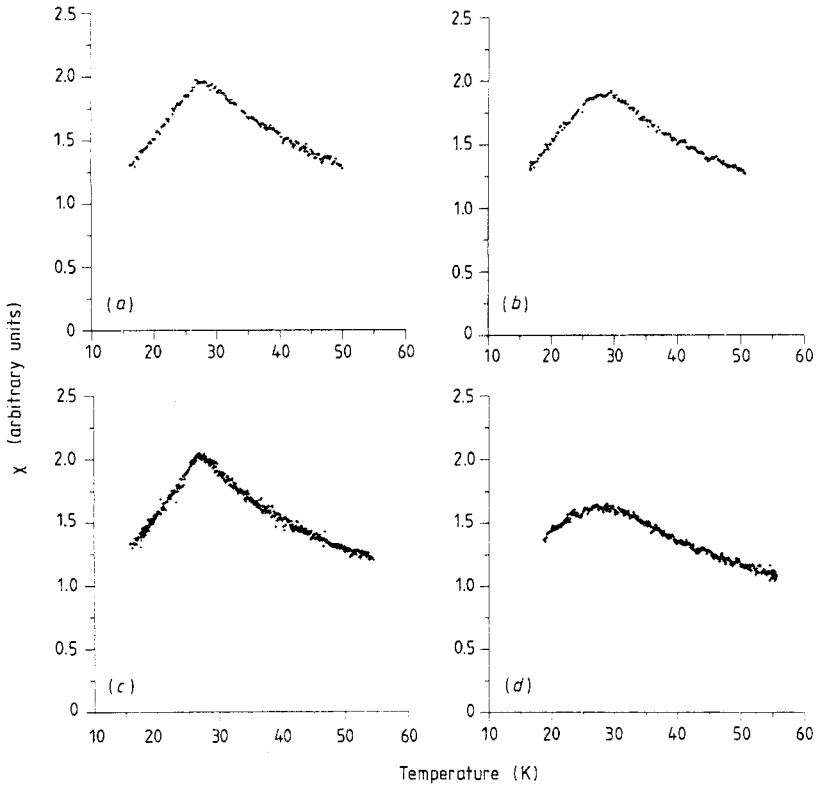

Figure 2. Graphs of susceptibility versus temperature for the alloy with $x = 0.25$ in (c) zero field and in applied fields of (a) 2 mT, (b) 4 mT and (d) 12 mT. Rounding of the cusp in the applied field is observed.

glass systems such as AuFe and $Eu_xSr_{1-x}S$ it is seen that T_f increases with increasing concentration of the magnetic species. In our series only the Fe atoms are magnetic and their concentration is constant but the values of susceptibility of the paramagnetic phase show that the moment per iron atom increases with x. Thus in our series increasing Fe magnetic moment is associated with increasing T_f. The effect of applied field on the cusp of the $x = 0.25$ alloy is shown in figure 2. A field ~ 10 mT smears out the sharp cusp to produce the rounded maximum observed, which is typical of spin glass behaviour.

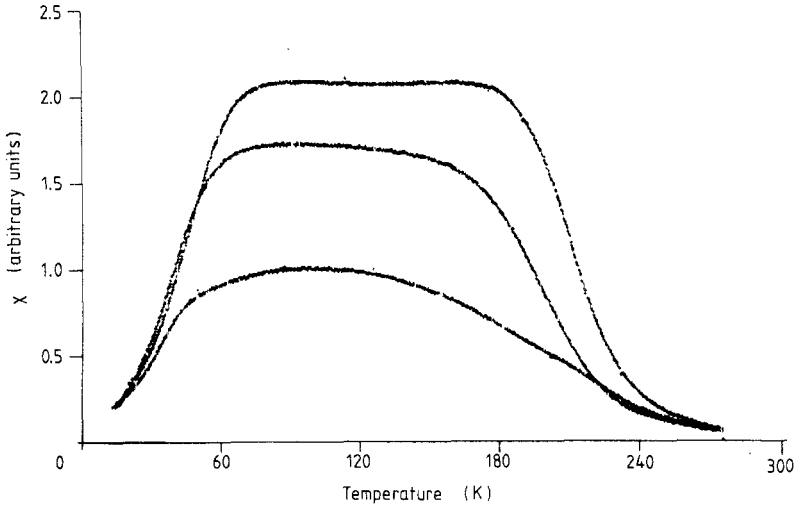

Figure 3. Graphs of susceptibility versus temperature for the alloy with $x = 0.325$ illustrating the re-entrant ferromagnetic phase. Transition temperatures T_f (magnetic glass to ferromagnetic phase) and T_c (ferromagnetic to paramagnetic phase) are taken from the positions where the modulus of the slope is greatest.

Susceptibility results for the $x = 0.325$ alloy in zero field and in applied fields of 2 mT and 10 mT are shown in figure 3, which illustrates typical results for a system which changes, with decreasing temperature, firstly from a paramagnetic to a ferromagnetic phase and then, at lower temperature, from a ferromagnetic to a magnetic glass phase. It thus illustrates the re-entrant ferromagnetic phase. Similar behaviour of χ_{AC} versus T is observed for other systems showing a re-entrant phase [4, 22]. The temperatures in table 1 corresponding to the paramagnetic to ferromagnetic transition T_c and for the ferromagnetic to magnetic glass transition T_f are taken at the maximum values of $|d\chi_{AC}/dT|$. The flat shape for the zero field χ_{AC} versus T graph of the ferromagnetic phase where χ_{AC} is very large has been attributed to a demagnetising limit [4]. In applied fields where domain movement is suppressed the value of susceptibility is reduced as expected. The shape of the χ versus T curves in applied field are consistent with those reported by Saleh *et al* [12].

3.2. Mössbauer results, variation of isomer shift δ with x

Room temperature spectra of some of the alloys studied are shown in figure 4. Fits to these spectra gave values of the isomer shift δ which are plotted against x in figure 5. It is seen that as the concentration of copper increases the value of the isomer shift decreases approximately linearly with x. This corresponds to a linear increase in the electron density at the iron nuclei. Extrapolation of the trend to $x = 0$ gives a value of $\delta = 0.27 \pm 0.01$ mm s^{-1}, consistent with the value of isomer shift for FeAl, $\delta = 0.28$ mm s^{-1} reported by Wertheim *et al* [3].

3.3. Variation in saturated hyperfine field $B_{HF}(0)$ with x

Spectra of the alloys recorded at 4.2 K are shown in figure 6. It is seen that they all exhibit distributions of hyperfine field. Histograms representing the fitted hyperfine field distributions $P(B_{HF})$ for the samples with $0.05 \leqslant x \leqslant 0.40$ are presented in figure 7.

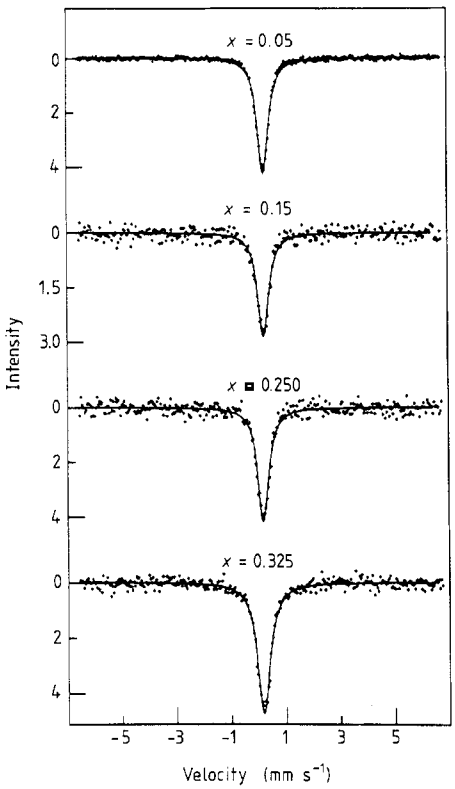

Figure 4. Mössbauer spectra taken at room temperature for alloys with $x = 0.05$, 0.15, 0.25 and 0.325. Isomer shift values are quoted with respect to metallic iron at room temperature.

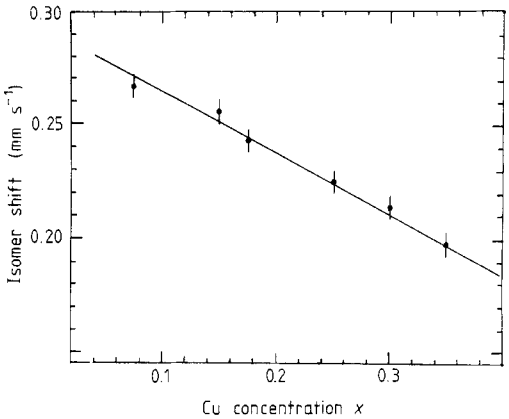

Figure 5. Graph of the isomer shift δ versus copper concentration x. The values of δ are obtained by fitting room temperature spectra, some of which are shown in figure 4.

These distributions show firstly that the mean saturated hyperfine field $\bar{B}_{HF}(0)$ increases with x and secondly that for the samples with $0.1 \leqslant x \leqslant 0.325$ the distributions are composed of two broad maxima with the intensity of the higher field maximum increasing at the expense of the lower field peak as the copper content x increases. Possible explanations for the shape of the distributions are discussed in section 4.3. In the distribution for the $x = 0.40$ sample, only the higher field peak is present.

3.4. Variation of Mössbauer ordering temperature T_{HF} with x

The room temperature spectrum of the alloy with $x = 0.40$ shows magnetic splitting indicating an ordering temperature above room temperature. The ordering temperatures of alloys in the range $0.01 \leqslant x \leqslant 0.325$ are below room temperature. Accurate determinations of the Mössbauer ordering temperature T_{HF} were made by the method of thermal scanning as described by Kobeissi [24] whereby the ratio of the centroid velocity transmission (CVT) was evaluated from the Mössbauer spectra where

CVT = Channel counts at velocity δ/Channel counts far from absorption.

Plots of CVT versus temperature are shown in figure 8. The values of T_{HF} are determined to an accuracy of ± 1 K for values $T_{HF} \leqslant 33$ K and to ± 2 K for the value of $T_{HF} = 273$ K which is in good agreement with the value found by Saleh *et al* [12].

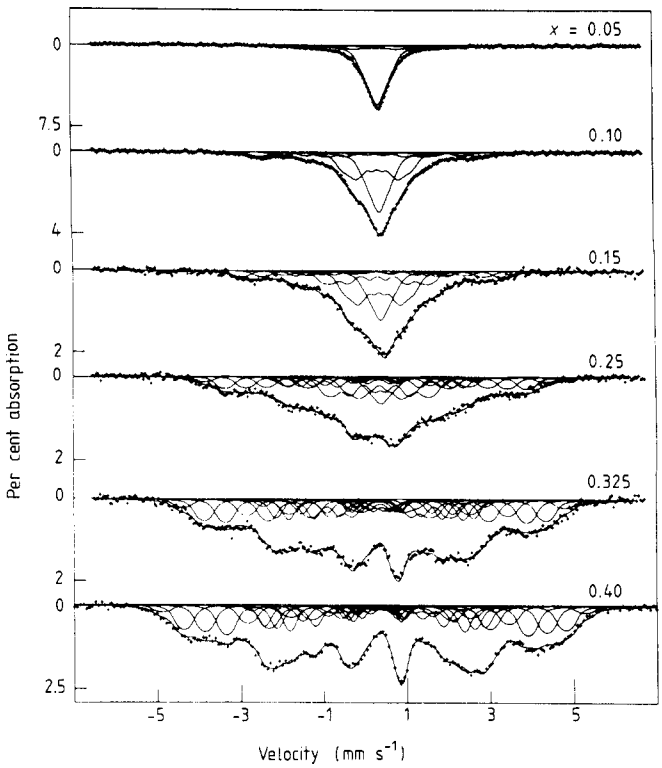

Figure 6. Mössbauer spectra of the complete range of $FeAl_{1-x}Cu_x$ alloys taken at 4.2 K. The spectra are fitted with a distribution of hyperfine fields.

The variation of T_{HF} with x is incorporated in the phase diagram of the alloy series shown in figure 9 and values of T_{HF} are listed in table 1. It is seen that the temperature of the phase boundary between paramagnetic and spin glass phases rises slowly with x but that a sharp rise in T_{HF} is seen when the ferromagnetic phase sets in.

4. Discussion

4.1. Magnetic susceptibility and phase diagram

The phase diagram shown in figure 9 is derived from the magnetic susceptibility results. In the range $0.15 \leqslant x \leqslant 0.25$ the sharp cusps observed in χ_{AC} versus T at zero applied field are characteristic of transitions between paramagnetic and spin glass phases, and mark the freezing temperature T_f. The rise in T_f with x corresponds to the increasingly magnetic nature of the alloys. The susceptibility versus temperature plots for the $x = 0.325$ alloy shown in figure 3 are typical of results identifying a re-entrant ferromagnetic phase between paramagnetic and magnetic glass phases. From our results the ferromagnetic phase sets in between $0.25 < x < 0.325$. The values of T_f listed in table 1 are consistent with values of $T_f = 20$ K for $x = 0.20$ and $T_f = 97$ K for $x = 0.30$ reported by Booth *et al* [16]. The sharp rise in the Mössbauer transition temperature T_{HF} for $x = 0.325$ is due to the setting in of this ferromagnetic phase. Comparison of the susceptibility and Mössbauer transition temperature listed in table 1 is discussed in section 4.5.

4.2. Dependence of iron cluster size upon copper content x

The random occupation of the iron and aluminium sites of the ordered FeAl structure by copper atoms results in some iron atoms occupying aluminium sites and thus forming

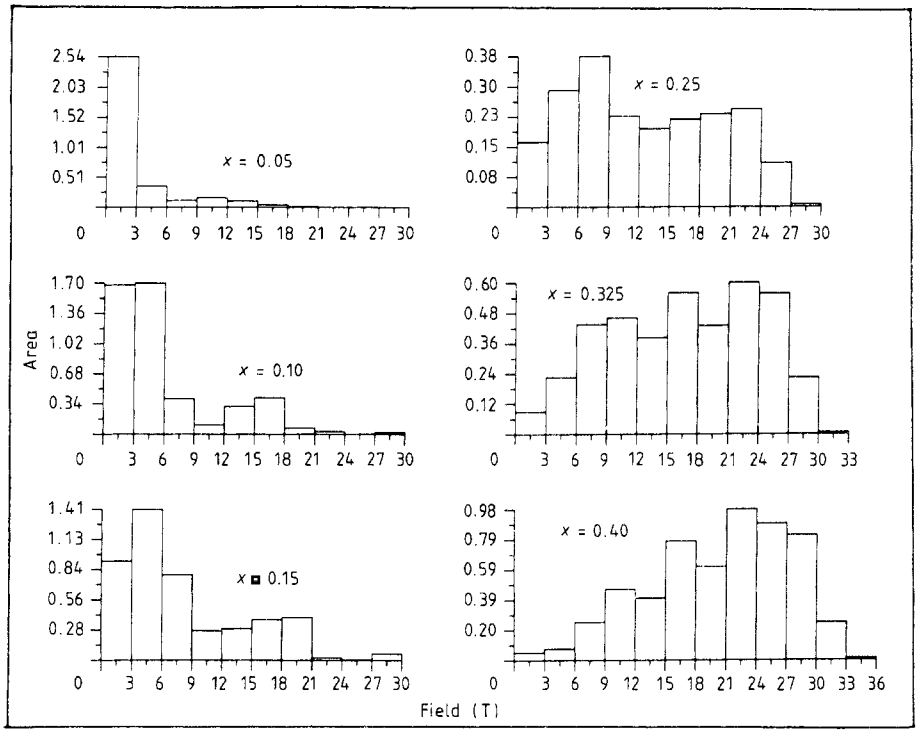

Figure 7. Distribution of hyperfine fields obtained from fitting the spectra of figure 6.

nearest neighbour iron networks or clusters. The size of these nearest neighbour clusters and the variation of this size with copper content x was investigated by a computer simulation technique. For a given value of x the $FeAl_{1-x}Cu_x$ structure was generated from the parent FeAl ordered structure by assuming that the copper atoms substitute randomly on sites 1 (Fe sites in FeAl) and sites 2 (Al sites in FeAl). In the simulation a random number generator assigns the copper atoms to sites such that:

(i) the probability for a site 1 or site 2 to be occupied by a copper atom is $x/2$;
(ii) the probability that a site 1 is occupied by an iron atom is $1 - x/2$;
(iii) the probability that a site 2 is occupied by an aluminium atom is $1 - x$;
(iv) the probability that a site 2 is occupied by an iron atom is $x/2$.

Equivalently if a copper atom substitutes for an aluminium atom on site 2, the iron sublattice is not affected but if a copper atom substitutes for an iron atom on site 1 then the displaced iron atom must eventually migrate to and remain on a site 2, resulting in the formation of iron atom clusters.

The size of the iron atom clusters generated by a given level of copper substitution was evaluated by selecting a central iron occupied site and counting all the nearest neighbour iron atoms in successive neighbour shells outwards. Checks for re-entrant paths were included. Simulations were computed for values of copper content $0 \leqslant x \leqslant 0.30$ for lattice sizes up to $49 \times 49 \times 49$ unit cells. Checks were made that the copper random substitutions matched the content level x and that the size of the lattice did not artificially limit the size of the clusters. The computations showed that the size of iron atom nearest neighbour clusters grew progressively faster as the copper content x increased. For a body centred lattice with iron atoms randomly distributed on the sites,

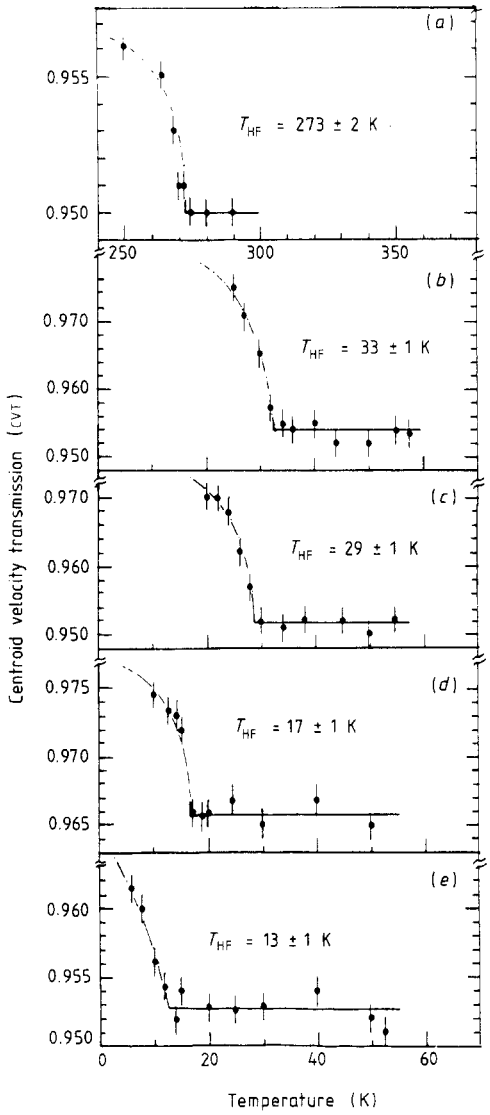

Figure 8. Results of the scanning technique to determine the Mössbauer transition temperatures T_{HF} for alloys with values of $x = (a)$ 0.325, (b) 0.25, (c) 0.225, (d) 0.15 and (e) 0.10.

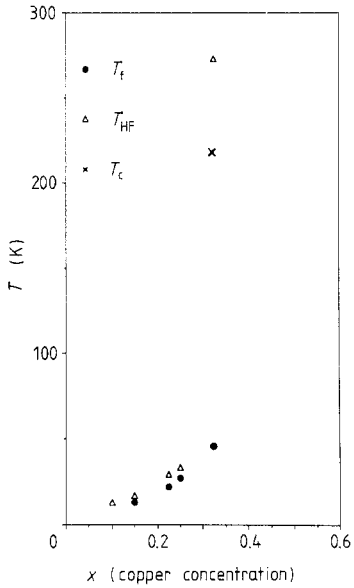

Figure 9. Phase diagram of the series $FeAl_{1-x}Cu_x$ constructed from the transition temperatures determined by the susceptibility and Mössbauer results of this study.

percolation theory predicts a cluster spanning the sample for a site occupation probability of $p_c = 0.24$. The cluster size equivalent to this in the computations above is reached at a copper content $x = 0.25$. However, the site occupation rules stated above are not equivalent to the random occupation of body centred cubic sites since for values of $x < 1$ a majority of iron atoms occupy sites 1. The effect of this will tend to inhibit the formation of percolating clusters in these alloys and will require values of $x > 0.25$ to form a cluster that spans the sample.

The identification of ferromagnetic order with a percolating cluster of nearest neighbour iron atoms arises from the observation that next nearest neighbour interactions between iron atoms in the structurally ordered alloy FeAl do not give rise to a ferromagnetic state. We thus interpret the calculation to expect that a ferromagnetic phase

should appear at a copper content $x \gtrsim 0.25$ causing the rise in T_c and T_{HF} with x that is observed.

4.3. Variation of isomer shift δ with x

Mössbauer spectra give information on the microscopic environment at the iron nuclei, the isomer shift compares the electron density at these sites. The copper to aluminium ratio changes the number of electrons in the conduction band. Taking the number of electrons released per atom to be in line with atomic valences, each copper atom can be regarded as releasing one electron into the conduction band and each aluminium atom as releasing three. Thus as x is increased across the range of alloy samples the density of conduction electrons falls. Following the values assumed above the conduction electron density should decrease linearly as x increases from $x = 0.05$ to 0.325. As the value x increases and the conduction electron density in the alloy samples decreases it is seen in figure 5 that the isomer shift falls approximately linearly with x throughout the whole range $0.05 \leqslant x \leqslant 0.325$. In the Mössbauer spectroscopy of ^{57}Fe larger electron density at the nucleus gives rise to smaller isomer shifts. Thus for the range of alloys the decrease in isomer shift with increasing x over the range $0 \leqslant x \leqslant 0.325$ indicates that at the iron nuclei the electron densities are progressively increasing; the increase being evaluated as 5×10^{-13} electrons per iron nuclear volume over the above range of x.

This apparent anomaly, that the isomer shifts indicate that the electron density at the iron nuclei increases while the number of electrons in the conduction band decreases, is accounted for by the change in occupation of the iron 3d shell. This 3d shell, lying energetically within the conduction band contains bound and virtually bound electrons. These 3d electrons act to screen the iron nucleus from the atomic 3s and possibly 4s electrons which contribute substantially to the electron density at the nucleus. Thus as x increases and the conduction electron density falls the occupation of the iron 3d shell falls and the 3s and 4s electron density at the nucleus rises causing the observed decrease of isomer shift.

An equivalent tendency was observed by Johnson *et al* [1] in the alloys $Fe_{2-y}Al_y$ ($0 \leqslant x \leqslant 0.2$) and by Stearns [2]. Increasing aluminium content caused an increase in isomer shift corresponding to a decrease in electron density at the iron sites.

4.4. Distributions of hyperfine field P(B_HF)

The distributions of hyperfine field shown in figure 7 from fitting the spectra of figure 6 show that:

(i) a broad distribution of hyperfine fields is necessary to fit the spectra of all the alloys with $x \geqslant 0.10$;

(ii) the mean value of the saturated hyperfine field $\bar{B}_{HF}(0)$ increases with x;

(iii) the distributions appear to be composed of broad maxima at values ~6 T and ~18 T with the intensity of the higher field maximum increasing at the expense of the lower field maximum as x increases.

In considering the increase of $\bar{B}_{HF}(0)$ with x, the dominant contact mechanism requires that the value of $B_{HF}(0)$ is proportional to the mean spin value $\langle S \rangle$ on the iron atoms. Thus as x increases and the electron density in the conduction band decreases, the value of $\langle S \rangle$ increases. The value of $\langle S \rangle$ is determined by the mean number of bound

or virtually bound electrons in the iron 3d shell. The isomer shift results require that the number of iron 3d electrons decreases as x increases. For these conditions to coexist with an increase of $B_{HF}(0)$ with x the mean number of 3d electrons on each iron atom must exceed five—at which value the 3d shell is half filled with electrons of parallel spin, which generates the maximum value of $\langle S \rangle$ and $B_{HF}(0)$. Thus for the aluminium rich alloys the mean number of iron 3d electrons is greatest but as the number of electrons in excess of five have opposite spin to the majority direction the value of $\langle S \rangle$ is reduced. As x increases the spin minority sense electrons are decreased and $\langle S \rangle$ and $\bar{B}_{HF}(0)$ increase. Thus the results of the isomer shift and the $\bar{B}_{HF}(0)$ variation with x require that the 3d shell on the iron atoms is more than half full. This discussion, which increased population of the iron 3d shell has the effect of decreasing the isomer shift δ and increasing the hyperfine field, indicates that in the fitting of the magnetic spectra of figure 6 the isomer shift δ_n of a component having hyperfine field $B_{HF}(n)$ should be of the form $\delta_n = \delta_0 - aB_{HF}(n)$ where a is a constant. This correlation was incorporated in the fits to the spectra of figure 6.

In order to account for the wide double peaked nature of the distributions in the range $0.10 \leqslant x \leqslant 0.325$ we note that Mössbauer studies of binary alloys [1, 2] show that the hyperfine field at a given atom is affected by the nature of its nearest neighbour atoms. The many different combinations of iron, aluminium and copper atoms that can surround each iron site in itself explains the spread of hyperfine field values. We associate the low field (~6 T) and higher field (~18 T) maxima of the distribution with iron atoms having few iron neighbours and mainly iron neighbours respectively. In terms of the iron networks or clusters discussed in section 4.2 iron atoms having comparatively few iron neighbours are likely to be situated in small clusters or on the outside of larger clusters. These iron sites would contribute to the low field maximum. Iron atoms near to the centre of large clusters are likely to have mainly iron nearest neighbours and to contribute to the higher field peak of the distribution. As the copper content x increases the size of the clusters increases and the proportion of iron atoms lying within them increases causing a growth of the higher field peak of the distribution at the expense of the lower field peak as seen in figure 7. For the $x = 0.40$ alloy effectively all iron atoms are connected in large clusters and only the higher field contributions are seen.

4.5. Mössbauer ordering temperature T_{HF}

Values of T_{HF}, the temperature at which the scanning technique detects a magnetic hyperfine field in the Mössbauer spectra are shown in the phase diagram of figure 9. It is seen that for copper content $0.15 \leqslant x \leqslant 0.25$ the values of $T_{HF} > T_f$, the freezing temperature measured by susceptibility. For $x = 0.325$ the Mössbauer transition temperature T_{HF} is again observed to be higher than the temperature T_c at which the AC susceptibility indicates the transition to the ferromagnetic phase. These differences in transition temperatures can be understood on the grounds that the Mössbauer technique detects a magnetic hyperfine field that is essentially static over a sensing time of 10^{-8} s. Thus iron atoms in the paramagnetic phase close to the freezing transition ($0.15 \leqslant x \leqslant 0.25$) or close to the ordering transition ($x = 0.325$) have relaxation times greater than the Mössbauer sensing time giving rise to a hyperfine field while still fluctuating fast with respect to the 15 Hz measurement of AC susceptibility. This behaviour, observed in this series as well as in other spin glass alloys [21] has not been found in several cases [22] and is thus not a general property of these magnetic systems.

The pronounced increase in T_{HF} for $x = 0.325$ and the onset of the ferromagnetic phase reflects the onset of a percolating cluster which is predicted for $x \geqslant 0.25$ as discussed in section 4.2.

Further experiments are planned to investigate further the magnetic phases and magnetic properties of this system in order to compare the measured results with the predictions of the theoretical models of such systems [9, 10].

Acknowledgments

We are indebted to Dr J G Booth of the University of Salford and to Dr A Saleh of Yarmouk University, Jordan for making the alloy samples available to us. SS wishes to acknowledge the support of an SERC research studentship and MAK wishes to thank the Department of Physics at the University of Liverpool for a pleasant and productive visit.

References

[1] Johnson C E, Ridout M S and Cranshaw T E 1963 *Proc. Phys. Soc.* **81** 1079
[2] Stearns M B 1964 *J. Appl. Phys.* **35** 1095
[3] Wertheim G K and Wernick J H 1967 *Acta Metall.* **15** 297
[4] Shull, R D, Okamoto H and Beck P A 1976 *Solid State Commun.* **20** 863
[5] Coles B R, Sarkissian B V B and Taylor R H 1979 *Phil. Mag.* B **37** 1685
[6] Nieuwenhuys G J, Verbeck B H and Mydosh J A 1979 *J. Appl. Phys.* **50** 1685
[7] Shukla P and Wortis M 1980 *Phys. Rev.* B **21** 159
[8] Grest G S 1980 *Phys. Rev.* **21** 165
[9] Gabay M and Toulouse G 1981 *Phys. Rev. Lett.* **47** 201
[10] Saslov W M and Parker G 1986 *Phys. Rev. Lett.* **56** 1074
[11] Okpalugo D E, Booth J G and Faunce C A 1985 *J. Phys. F: Met. Phys.* **15** 681, 2025
[12] Saleh A S, Mankikar R M, Yoon S, Okpalugo D E and Booth J G 1985 *J. Appl. Phys.* **57** 3241
[13] Perez Alcazar G A, Plascak J A and Galvao de Silva E 1986 *Phys. Rev.* B **34** 1940
[14] Helio Chachem and Galvao de Silva E 1987 *Phys. Rev.* **35** 1602
[15] Goldfarb R B, Rao K V and Chen H S 1985 *Solid State Commun.* **54** 799
[16] Booth J G, de Boer F R and Huang Ying-Kai 1988 *J. Physique Coll.* **49** C8 145
[17] Ait-Bahamon A, Meyer C, Hartmann-Boutron F, Gros Y, Campbell I A, Jeanday C and Oddon J L 1988 *J. Physique Coll.* **49** C8 1075
[18] Huck B, Iandes L, Stasch R and Hesse J 1988 *J. Physique Coll.* **49** C8 1141
[19] Lauer J and Keune W 1982 *Phys. Rev. Lett.* **48** 1850
[20] Huang C Y 1985 *J. Magn. Magn. Mater.* **51** 1
[21] Meyer C, Hartmann-Boutron F, Gros Y and Campbell I A 1985 *J. Magn. Magn. Mater.* **46** 254
[22] Moorjani K and Coey J M D 1984 *Magnetic Glasses* (Amsterdam: Elsevier) p 329
[23] Pickart J and Nathans R 1961 *Phys. Rev.* **123** 1163
[24] Kobeissi M A 1981 *Phys. Rev.* B **24** 2380